The role of LAT1 in ^{18}F-DOPA uptake in malignant gliomas

Ryan S. Youland, **Gaspar J. Kitange**, **Timothy E. Peterson**, **Deanna H. Pafundi**, **Judi A. Ramiscal**, **Jenny L. Pokorny**, **Caterina Giannini**, **Nadia N. Laack**, **Ian F. Parney**, **Val J. Lowe**, **Debra H. Brinkmann**, and **Jann N. Sarkaria**

College of Medicine, Mayo Clinic, 200 First Street SW, Rochester, MN 55905, USA

Department of Radiation Oncology, Mayo Clinic, 200 First Street SW, Rochester, MN 55905, USA

Department of Neurosurgery, Mayo Clinic, 200 First Street SW, Rochester, MN 55905, USA

Department of Pathology, Mayo Clinic, 200 First Street SW, Rochester, MN 55905, USA

Department of Radiology, Mayo Clinic, 200 First Street SW, Rochester, MN 55905, USA

Abstract

Positron emission tomography (PET) imaging with the amino acid tracer 6-^{18}F-fluoro-ʟ-3,4-dihydroxy-phenylalanine (^{18}F-DOPA) may provide better spatial and functional information in human gliomas than CT or MRI alone. The ʟ-type amino acid transporter 1 (LAT1) is responsible for membrane transport of large neutral amino acids in normal cells. This study assessed the relationship between LAT1 expression and ^{18}F-DOPA uptake in human astrocytomas. Endogenous LAT1 expression was measured in established glioblastoma (GBM) cell lines and primary GBM xenografts using Western blotting and quantitative reverse transcription polymerase chain reaction (qRT-PCR). Uptake of ^{18}F-DOPA was approximated in vitro using [3]H-ʟ-DOPA as an analog. Uptake of [3]H-ʟ-DOPA was assessed in cells expressing LAT1 shRNA or LAT1 siRNA and compared to non-targeted (NT) control shRNA or siRNA sequences, respectively. To demonstrate the clinical relevance of these findings, LAT1 immunofluorescence staining was compared with corresponding regions of ^{18}F-DOPA PET uptake in patients with newly diagnosed astrocytomas. LAT1 mRNA and protein expression varies in GBM, and the extent of [3]H-ʟ-DOPA uptake was positively correlated with endogenous LAT1 expression. Stable shRNA-mediated LAT1 knockdown in T98 and GBM28 reduced [3]H-ʟ-DOPA uptake relative to NT shRNA by 57 ($P < 0.0001$) and 52 % ($P < 0.001$), respectively. Transient siRNA-mediated LAT1 knockdown in T98 reduced [3]H-ʟ-DOPA uptake relative to NT siRNA up to 68 % ($P < 0.01$). In clinical samples, LAT1 expression positively correlated with ^{18}F-DOPA PET uptake ($P = 0.04$). Expression of LAT1 is strongly associated with [3]H-ʟ-DOPA uptake in vitro and ^{18}F-DOPA uptake in patient biopsy samples. These results define LAT1 as a key determinant of ^{18}F-DOPA accumulation in GBM.

Keywords

^{18}F-DOPA PET/CT; Glioma; Glioblastoma; Amino acid transport

---

Youland.Ryan@Mayo.eduSarkaria.Jann@Mayo.edu.

Introduction

Positron emission tomography (PET)-CT allows a functional evaluation of metabolic perturbations unique to cancer, and this provides an opportunity to delineate normal and tumor tissue based on functional PET imaging. Specifically for imaging brain tumors, 6-^{18}F-fluoro-L-3,4-dihydroxy-phenylalanine (^{18}F-DOPA) is a promising radi-otracer with high uptake in malignant brain tumors and low uptake in normal brain tissue [1]. In comparison to the radiotracers 2-deoxy-2-^{18}F-fluoro-D-glucose (^{18}F-FDG) or 3-deoxy-3-^{18}F-fluorothymidine (^{18}F-FLT), ^{18}F-DOPA provides more accurate visualization of high-grade, low-grade, and recurrent tumors [2, 3]. Thus, there is significant interest in using ^{18}F-DOPA PET in conjunction with traditional magnetic resonance imaging (MRI) for neurosurgical and radiation therapy planning in gliomas [4].

The mechanism associated with elevated ^{18}F-DOPA accumulation in gliomas has not been established, although up-regulation of an ^{18}F-DOPA transporter may contribute to this phenotype [5]. The L-type amino acid transporter 1 (LAT1) is a sodium-independent neutral amino acid transporter that facilitates L-DOPA transport in renal epithelial cells and endothelial cells in brain capillaries [6-9], as well as L-methyl-^{11}C-methionine (^{11}C-MET) in human gliomas [10]. High LAT1 expression has been shown to correlate with tumor grade and potentially lower survival in human astrocytomas [11, 12]. Based on these data, the current study evaluated the influence of LAT1 on ^{18}F-DOPA accumulation in human astrocytomas in both in vitro studies and in human biopsy samples.

Materials and methods

Cells and reagents

Primary serially transplantable GBM xenografts were established as previously described, and along with U87 and T98 glioma cell lines, were thawed from frozen stocks [13]. Cells were grown in tissue culture flasks containing DMEM medium (Gibco Life Technologies, Carlsbad, CA) supplemented with 10 % fetal bovine serum (Invitrogen, Carlsbad, CA) and 1 % penicillin/streptomycin (100 U/mL; Gibco).

Western blotting for LAT1

Antibodies were purchased targeting human LAT1 (poly-clonal; Cell Signaling Technology, Beverly, MA) and human ß-Actin (monoclonal; Sigma-Aldrich, St. Louis, MO). Cells were lysed in a detergent-containing buffer [20 mM Tris–HCl (pH 7.4), 0.1 % sodium dodecyl sulfate (SDS), 1 % Triton X-100, and 1 % sodium deoxycholate] with protease inhibitors (Roche, Indianapolis, IN). Lysates were prepared, resolved by electrophoresis, and transferred to nitrocellulose membranes as described previously [14]. Nonspecific binding was blocked with 5 % nonfat milk, 0.1 % Tween-20 and 50 mM Tris (TBST, pH 7.5). Primary antibodies were prepared according to the manufacturer's instructions and incubated overnight at 4 °C. Secondary antibodies (horseradish-peroxidase-conjugated anti-IgG; Pierce, Rockford, IL) were incubated for 1 h at room temperature. Membranes were developed using the Pierce chemiluminescence protocol (Pierce), stripped, and incubated with an anti-ß-actin antibody to confirm even sample loading.

RNA isolation, reverse transcription and quantitative RT-PCR (qRT-PCR)

Total cellular RNA was isolated with the RNeasy kit (QIAGEN, Valencia, CA). RNA concentrations were determined by spectrophotometry at 260 nm using a Nano-Drop 2000 (Thermo Scientific, Wilmington, DE). Reverse transcription was performed using 2 μg of RNA, synthesized to cDNA in a 20 μL reaction system with reverse transcriptase (RT), RT

buffer, and random primers (Promega, Madison, WI). Conditions for reverse transcription were 5 min at 70 °C, 5 min on ice and then 90 min at 37 °C.

Oligodeoxynucleotide primers were purchased for PCR amplification (Integrated DNA Technologies, Coralville, IA); LAT1: forward (5′-CCCAACTTCTCATTTGAAGGCACC-3′) and reverse (5′-CCATAGCGAAAGAGGCCGCTGTATAA-3′) and ß-actin: forward (5′-CCAGAGATGGCCACGGCTGCT-3′) and reverse (5′-TCCTTCTGGATCCTGTCGGGA-3′). The qRT-PCR was performed on an ABI Prism 7900 with 384-well plates using adhesive seals as covers. PCR mixes were created for LAT1 and the ß-actin endogenous control in a 20 μL reaction per well using a single-step qRT-PCR reagent kit (ABI). The qRT-PCR was programmed as follows: 30 min at 42 °C, 10 min at 95 °C, then 40 cycles of 15 s at 95 °C then 1 min at 60 °C. Each sample was amplified in triplicate. Relative levels of LAT1 mRNA were calculated using the SDS RQ 1.3 software (ABI).

Stable shRNA-mediated knockdown of LAT1

A LAT1-targeted shRNA expressing pGIPZ plasmid was used with the sequence 5′-TGCTGTTGACAGTGAGCGCGGTACGAATCTCATCCCTCAATAGTGAAGCCACAG ATGTATTGAGGGATGAGATTCGTACCATGCCTACTGCCTCGGA-3′ (Open Biosystems, Huntsville, AL) and a non-specific targeting (NT) shRNA for control. Plasmid-containing bacteria were amplified per the manufacturer's protocol. Plasmids were isolated and purified using the HiSpeed Plasmid Midi Kit (QIAGEN). Lentiviral packaging was performed with Trans-Lentiviral packaging mix in 293T cells according to the manufacturer's instructions (Open Biosystems).

T98 and GBM28 cells were plated on 6-well plates at 1×10^5 and 2×10^5 cells per well, respectively. The following day, medium was aspirated and replaced with 750 μL of medium with 10 μg/mL polybrene. Next, 250 μL of virus-containing solution was added to each well and incubated at 37 °C for 24 h. Cells were selected with puromycin and monitored for GFP expression.

Small interfering RNA knockdown of LAT1

The 27-nt TriFECTa siRNA kit for human LAT1 was designed and provided by IDT. Three different siRNA sequences targeting LAT1 were used: siRNA #1 had the sequence: 5′-CCUAUGGAGGAUGGAAUU-3′ (sense) and 5′-UUCAAGUAAUUCCAUCCU-3′ (antisense); siRNA #2: 5′-GGACAUGCCUCAAGGAUA-3′ (sense) and 5′-CUCCCUGUAUCCUUGAGG-3′ (antisense); siRNA #3: 5′-UCUAGAAACAGAGACAAG-3′ (sense) and 5′-UGCCUUUCUUGUCUCUGU-3′ (antisense). Negative control siRNA was provided by IDT. T98 cells were transfected with 25 nM of siRNA using instructions provided with HiPerFect reagent (QIAGEN). Cells were processed in parallel for Western blotting and assessment of ^{3}H-L-DOPA uptake at 72 h.

Cellular uptake of ^{3}H-L-DOPA

Cells were plated in 24-well plates (1×10^4 cells/mL) and ^{3}H-L-DOPA uptake studies were performed at 48 h. A sodium-free uptake solution (US) was created containing 125 mM choline chloride, 5.6 mM D-glucose, 4.8 mM KCl, 1.2 mM $MgSO_4$, 1.2 mM KH_2PO_4, 1.3 mM $CaCl_2$ and 25 mM HEPES (pH of 7.4). For experiments, standard medium was aspirated and cells were washed gently three times with 500 lμL US and pre-incubated with 500 μL of US for 10 min. US was aspirated and 500 μL of buffer was added containing 10 μM L-DOPA (Sigma) and 18.5 kBq of ^{3}H-L-DOPA (Moravek Biochemicals, Brea, CA) per well. After 20 min of incubation at 37 °C, uptake was terminated by washing cells with 500

μL ice cold buffer three times. Cells were lysed by incubating in 0.3 M NaOH with 0.1 % Triton-X for 20 min at room temperature. Lysate was added to an equal volume of liquid scintillation fluid and quantified with a liquid scintillation counter. Radioactive content of the lysate was adjusted for protein content by quantitating protein with the Bradford method. Differences in ^{3}H-L-DOPA uptake in relation to LAT1 expression were analyzed using a two-sample *t* test.

Patients, ^{18}F-DOPA synthesis, PET acquisition and data analysis

As part of a prospective imaging/biopsy study at Mayo Clinic in Rochester, Minnesota taking place between October 2010 and September 2011, 6 patients (5 men, 1 woman) with newly diagnosed astrocytomas were included. All patients provided written informed consent prior to participation, and the study was approved by the Mayo Clinic Institutional Review Board. The details of the protocol and results for all patients studied are being reported elsewhere (Pafundi et al. manuscript submitted).

Prior to surgery, patients had a PET/CT scan, followed by an MRI (GE Signa HDxt® 1.5 Tesla) with contrast. PET imaging was performed with a GE Discovery 690® PET/CT system. ^{18}F-DOPA (5.0 ± 10 % mCi) was administered intravenously and 10 min after injection, a 10 min 3-dimensional (3D) PET acquisition was performed and a 47-slice helical CT pre-scan image was obtained for attenuation correction of PET data. PET sinograms were reconstructed with a fully ordered-subset expectation maximization (3D-OSEM) algorithm.

The ^{18}F-DOPA PET scan was registered to intra-operative or pre-operative T1- and T2-weighted MRI scans using MIM Maestro™ (MIM Software, Cleveland, OH) and transferred to the Stealth Station™ Neuronavigation System (Medtronic Sofamor Danek, Memphis, TN). Subsequently, 1 to 3 locations of PET and MRI concordance and discordance were stereotactically biopsied for each patient during the course of resection. A 10 mm diameter region of interest (ROI) was selected around each biopsy coordinate and analyzed for median tumor standardized uptake value (SUVmedian) by an experienced radiation physicist.

LAT1 immunofluorescence

A Mayo Clinic neuropathologist evaluated the H&E stained biopsy samples according to World Health Organization criteria and defined sections with suitable tissue for LAT1 analysis. Formalin-fixed paraffin embedded sections were deparaffinized with xylene and rehydrated with a series of alcohol washes. Antigen retrieval was performed using 10 mM sodium citrate (pH 6.0) for 30 min. Samples were blocked with 10 % goat serum in PBS supplemented with 0.1 % Tween-20 for 30 min at room temperature. Anti-LAT1 (Epitomics, Burlingame, CA) primary antibody was added at a concentration of 1:100 and incubated for 2 h at room temperature. After washing, samples were incubated with a secondary Cy5-labeled antibody and counterstained with DAPI (4,6,-diamidino-2-phenylindole). The slides were visualized using a Zeiss LSM 510 confocal laser scanning microscope and LAT1 expression was semi-quantitatively graded according to the following system: (−) for no LAT1 expression, (+) for minimal staining, (++) for patchy, moderately diffuse staining, and (+++) for widely diffuse LAT1 staining. Correlation between ^{18}F-DOPA PET SUVmedian and LAT1 expression was performed using the Mann–Whitney *U* test.

Results

Endogenous LAT1 expression and ^{3}H-L-DOPA uptake in human glioma lines

LAT1 expression was evaluated in a panel of five human glioma cell lines by Western blotting and qRT-PCR. One established cell line (T98) and two primary xenograft lines (GBM22 and GBM28) had readily detectable LAT1 and one established cell line (U87) and one primary xenograft line (GBM6) had relatively low LAT1 expression (Fig. 1a, b). Specifically, LAT1 expression was significantly lower in U87 (16 % of T98 expression, $P <$ 0.001; 14 % of GBM28, $P <$ 0.01) and GBM6 (14 % of T98, $P <$ 0.001; 12 % of GBM28, $P <$ 0.05). Corresponding with the low LAT1 expression in these two lines, ^{3}H-L-DOPA uptake was significantly lower in U87 (26 % of T98 uptake, $P <$ 0.001; 33 % of GBM28, $P <$ 0.05) and GBM6 (28 % of T98, $P <$ 0.01; 35 % of GBM28, $P <$ 0.01; Fig. 1c). To summarize, GBM cell lines with low LAT1 expression had significantly less ^{3}H-L-DOPA uptake as compared to cell lines with readily detectable LAT1.

Knockdown of LAT1 reduces ^{3}H-L-DOPA uptake in human glioma lines

The influence of LAT1 expression on L-DOPA uptake was specifically investigated using RNA interference-mediated LAT1 knockdown in both T98 and GBM28 cells. Lentiv-irally delivered shRNA significantly reduced LAT1 protein expression (Fig. 2a). At the mRNA level, LAT1 shRNA reduced LAT1 expression by 83 % in T98 ($P <$ 0.001) and 74 % in GBM28 ($P <$ 0.001) as compared to the NT shRNA control (Fig. 2b). Knockdown of LAT1 expression was associated with a significantly lower ^{3}H-L-DOPA uptake by 57 % in T98 ($P <$ 0.0001) and 52 % in GBM28 ($P <$ 0.001, Fig. 2c). To compliment the shRNA data, LAT1 RNA interference was performed in T98 using three different siRNA oligonucleotide sequences. Significant reaching maximal knockdown at 72 h (Fig. 3a). Relative to NT siRNA control-treated samples, ^{3}H-L-DOPA uptake was reduced by 58 % in siRNA #1 ($P =$ 0.07), 68 % in siRNA #2 ($P =$ 0.007), and 58 % in siRNA #3 ($P =$ 0.03; Fig. 3b). These results demonstrate that LAT1 is an important mediator of ^{3}H-L-DOPA uptake in GBM in vitro.

Correlation of ^{18}F-DOPA uptake with LAT1 expression in patient astrocytoma tissue

The relationship between LAT1 expression and ^{18}F-DOPA uptake was further explored as part of a larger ^{18}F-DOPA imaging study in which image-guided biopsy samples were obtained from regions of different ^{18}F-DOPA uptake in patients with newly diagnosed astrocytomas (Fig. 4a). Pathologic review of the biopsy samples defined 2 patients with grade II (4 samples), 2 with grade III (4 samples), and 2 with grade IV (4 samples) astrocytomas, for a total of 12 unique biopsy samples in 6 patients. LAT1 immunofluorescence was performed on all 12 biopsy samples (Fig. 4b, c). Semi-quantitative LAT1 expression scoring revealed no (−) staining in one, (+) staining in five, (++) staining in four, and (+++) staining in two samples. There was a marginally significant trend toward increasing LAT1 expression with higher pathologic grade ($P =$ 0.054). Median SUV from the biopsy region for these 12 biopsy sites ranged from 0.93 to 3.68. Analysis with the Mann–Whitney U test revealed a statistically significant positive correlation between ^{18}F-DOPA PET SUVmedian and LAT1 expression (Fig. 5; $P =$ 0.04). These findings confirm the potential importance of LAT1 as a mediator of ^{18}F-DOPA uptake in newly diagnosed astrocytomas.

Discussion

PET imaging is commonly used in oncology to accurately define tumor extent in a wide variety of malignancies. While ^{18}F-FDG is a frequently used PET tracer, the high rate of glucose metabolism in normal brain results in a high background of FDG uptake that limits

its utility for imaging brain tumors [15]. In comparison, amino acid-based radiotracers, such as ^{11}C-MET or ^{18}F-DOPA have relatively low brain uptake compared to tumor uptake, and there is significant interest in using these novel radiotracers to more accurately define tumor extent in conjunction with traditional MR imaging [2, 16]. Specifically, our group and others have demonstrated that regions of detectable ^{18}F-DOPA PET uptake can extend significantly beyond the T1 with contrast or T2/FLAIR volumes [1-3, 17]. The focus of the current study was to define whether LAT1 influences tumor uptake of ^{18}F-DOPA. Expression levels of LAT1 in human glioma cell lines and patient tumor biopsies varied significantly, but positively correlated with ^{3}H-L-DOPA and ^{18}F-DOPA uptake, respectively. Moreover, shRNA and siRNA knockdown of LAT1 significantly suppressed ^{3}H-L-DOPA uptake in vitro. Collectively, these data suggest LAT1 as an important transporter of ^{18}F-DOPA in human astrocytomas.

LAT1 is an important mediator of large neutral amino acid transport across cell membranes. LAT1 is expressed in the endothelial cells comprising the blood–brain barrier to facilitate uptake of neutral amino acids into brain tissue [6], but overall expression is quite low in normal brain [11, 12]. In comparison, LAT1 expression levels correlate with tumor grade for astrocytomas, which may reflect the increased cellular demands for amino acids associated with rapid tumor growth [10-12]. Previous studies have correlated LAT1 expression with uptake of ^{11}C-MET and ^{14}C-L-leucine in human gliomas [10, 18], and L-DOPA, L-leucine, and other large neutral amino acids in various normal tissues [6-8, 19]. The current study is the first to clearly link LAT1 function to the level of ^{3}H-L-DOPA and ^{18}F-DOPA accumulation in gliomas. These data suggest that changes in LAT1 expression can have a significant impact on ^{18}F-DOPA uptake in clinical PET imaging. Nonetheless, there are likely additional factors that drive ^{18}F-DOPA uptake and retention within cells. Despite robust knockdown of LAT1 expression in T98 and GBM28 cells, ^{3}H-L-DOPA uptake was only reduced by approximately 50–70 %. Similarly, in previous studies, approximately 90 % suppression of LAT1 mRNA levels lowered melphalan influx only by 58 % in HeLa cells and ^{14}C-L-leucine uptake by 58 % in KB oral cancer cells [20, 21]. Radiotracer accumulation within cells reflects both transport across the cellular membrane and then subsequent metabolism to trap the tracer within the cell. While a detailed analysis of ^{18}F-DOPA metabolites and their function is beyond the scope of this paper, ^{18}F-DOPA is converted to ^{18}F-dopamine, which may be retained in synaptic vesicles [22] or converted to 3-*O*-Methyl-6-^{18}F-fluoro-L-DOPA (OFMD) [22, 23]. Although metabolites have the potential to confound our results, the effect is unlikely to be significant, as OFMD has similar uptake in brain tumors to other ^{18}F-labeled amino acids [24]. Subsequent metabolites are decarboxylated and eventually lost via diffusion [22]. The minimal persistent accumulation of ^{18}F-DOPA in the current experiment might simply relate to residual LAT1 activity within the cell membrane or alternate transport mechanisms, such as paracellular diffusion [25] or activity of other amino acid transporters (LAT2) [26], in conjunction with cellular L-DOPA metabolism that captures any ^{18}F-DOPA that is effectively transported across the membrane [7]. Additional studies are required to clearly define all the components that mediate ^{18}F-DOPA uptake in human gliomas.

Defining the relationship between LAT1 activity and ^{18}F-DOPA accumulation provides an important mechanistic link that can provide insight into biochemical factors that influence the performance of ^{18}F-DOPA imaging in tumors. There was a non-statistically significant trend in the present study between LAT1 expression and tumor grade consistent with prior reports that LAT1 expression correlates with tumor grade, proliferation, and poor prognosis in many tumors including gliomas [10-12, 27-34]. Consistent with these data, regions of high ^{18}F-DOPA uptake correlate with glioma grade in a larger study being conducted at Mayo Clinic (Pafundi et al. manuscript submitted). High-grade gliomas have extensive regions of hypoxia, and previous studies provide conflicting data regarding the influence of

hypoxia on LAT1 expression [35, 36]. Additional biochemical studies suggest that mammalian target of rapamycin (mTOR), protein kinase C, platelet derived growth factor, and androgen receptor signaling also can drive LAT1 expression. Conversely, LAT1-mediated uptake of essential amino acids is important for robust mTOR activation in tumors [37-39]. In light of the high level of LAT1 expression observed in many tumors, several groups are exploring the therapeutic utility of cytotoxic LAT1 substrates [40-42]. Within the context of these studies, our data demonstrating a mechanistic link between LAT1 expression and ^{18}F-DOPA uptake suggest that ^{18}F-DOPA imaging could be used to evaluate signaling inhibitors that influence LAT1 expression or to select tumors for use of LAT1-based novel therapeutic strategies.

Conclusion

This study demonstrates that LAT1 expression significantly correlated with ^{3}H-L-DOPA uptake in human gliomas in vitro and ^{18}F-DOPA uptake in vivo. These results are the first report of a relationship between ^{18}F-DOPA uptake and LAT1 expression in human gliomas. As additional factors driving LAT1 expression and other mediators of ^{18}F-DOPA transport are discovered, these data will provide researchers a more clear understanding of how ^{18}F-DOPA PET can be optimally deployed in the field of oncology.

Acknowledgments

References

1. Ledezma CJ, Chen W, Sai V, Freitas B, Cloughesy T, Czernin J, Pope W. ^{18}F-FDOPA PET/MRI fusion in patients with primary/recurrent gliomas: initial experience. Eur J Radiol. 2009; 71:242–248. doi:10.1016/j.ejrad.2008.04.018. [PubMed: 18511228]

2. Chen W, Silverman DH, Delaloye S, Czernin J, Kamdar N, Pope W, Satyamurthy N, Schiepers C, Cloughesy T. 18F-FDOPA PET imaging of brain tumors: comparison study with 18F-FDG PET and evaluation of diagnostic accuracy. J Nucl Med. 2006; 47:904–911. [PubMed: 16741298]

3. Tripathi M, Sharma R, D'Souza M, Jaimini A, Panwar P, Varshney R, Datta A, Kumar N, Garg G, Singh D, Grover RK, Mishra AK, Mondal A. Comparative evaluation of F-18 FDOPA, F-18 FDG, and F-18 FLT-PET/CT for metabolic imaging of low grade gliomas. Clin Nucl Med. 2009; 34:878–883. doi:10.1097/RLU.0b013e3181becfe0. [PubMed: 20139821]

4. Walter F, Cloughesy T, Walter MA, Lai A, Nghiemphu P, Wagle N, Fueger B, Satyamurthy N, Phelps ME, Czernin J. Impact of 3,4-dihydroxy-6-18F-fluoro-l-phenylalanine PET/CT on managing patients with brain tumors: the referring physician's perspective. J Nucl Med. 2012; 53:393–398. doi:10.2967/jnumed.111.095711. [PubMed: 22323780]

5. Schiepers C, Chen W, Cloughesy T, Dahlbom M, Huang SC. 18F-FDOPA kinetics in brain tumors. J Nucl Med. 2007; 48:1651–1661. doi:10.2967/jnumed.106.039321. [PubMed: 17873130]

6. Kageyama T, Nakamura M, Matsuo A, Yamasaki Y, Takakura Y, Hashida M, Kanai Y, Naito M, Tsuruo T, Minato N, Shimohama S. The 4F2hc/LAT1 complex transports l-DOPA across the blood-brain barrier. Brain Res. 2000; 879:115–121. [PubMed: 11011012]

7. del Amo EM, Urtti A, Yliperttula M. Pharmacokinetic role of l-type amino acid transporters LAT1 and LAT2. Eur J Pharm Sci. 2008; 35:161–174. doi:10.1016/j.ejps.2008.06.015. [PubMed: 18656534]

8. Pinho MJ, Serrao MP, Gomes P, Hopfer U, Jose PA, Soares-da-Silva P. Over-expression of renal LAT1 and LAT2 and enhanced l-DOPA uptake in SHR immortalized renal proximal tubular cells. Kidney Int. 2004; 66:216–226. doi:10.1111/j.1523-1755.2004.00722.x. [PubMed: 15200428]

9. Kanai Y, Segawa H, Miyamoto K, Uchino H, Takeda E, Endou H. Expression cloning and characterization of a transporter for large neutral amino acids activated by the heavy chain of 4F2 antigen (CD98). J Biol Chem. 1998; 273:23629–23632. [PubMed: 9726963]

10. Okubo S, Zhen HN, Kawai N, Nishiyama Y, Haba R, Tamiya T. Correlation of l-methyl-11C-methionine (MET) uptake with l-type amino acid transporter 1 in human gliomas. J Neurooncol. 2010; 99:217–225. doi:10.1007/s11060-010-0117-9. [PubMed: 20091333]

11. Kobayashi K, Ohnishi A, Promsuk J, Shimizu S, Kanai Y, Shiokawa Y, Nagane M. Enhanced tumor growth elicited by l-type amino acid transporter 1 in human malignant glioma cells. Neurosurgery. 2008; 62:493–503. doi:10.1227/01.neu.0000316018. 51292.19 discussion 503-494. [PubMed: 18382329]

12. Nawashiro H, Otani N, Shinomiya N, Fukui S, Ooigawa H, Shima K, Matsuo H, Kanai Y, Endou H. l-type amino acid transporter 1 as a potential molecular target in human astrocytic tumors. Int J Cancer. 2006; 119:484–492. doi:10.1002/ijc.21866. [PubMed: 16496379]

13. Giannini C, Sarkaria JN, Saito A, Uhm JH, Galanis E, Carlson BL, Schroeder MA, James CD. Patient tumor EGFR and PDGFRA gene amplifications retained in an invasive intracranial xenograft model of glioblastoma multiforme. Neuro Oncol. 2005; 7:164–176. doi:10.1215/S1152851704000821. [PubMed: 15831234]

14. Kitange GJ, Carlson BL, Schroeder MA, Grogan PT, Lamont JD, Decker PA, Wu W, James CD, Sarkaria JN. Induction of MGMT expression is associated with temozolomide resistance in glioblastoma xenografts. Neuro Oncol. 2009; 11:281–291. doi:10.1215/15228517-2008-090. [PubMed: 18952979]

15. Strauss LG. Fluorine-18 deoxyglucose and false-positive results: a major problem in the diagnostics of oncological patients. Eur J Nucl Med. 1996; 23:1409–1415. [PubMed: 8781149]

16. Hatakeyama T, Kawai N, Nishiyama Y, Yamamoto Y, Sasakawa Y, Ichikawa T, Tamiya T. 11C-methionine (MET) and ^{18}F-fluorothymidine (FLT) PET in patients with newly diagnosed glioma. Eur J Nucl Med Mol Imaging. 2008; 35:2009–2017. doi:10.1007/s00259-008-0847-5. [PubMed: 18542957]

17. Pafundi DH, Brinkmann DH, Parney IF, Giannini C, Laack NN, Kemp B, Lowe V, Sarkaria JN, Yan ES. Biopsy validation of (18)F-FDOPA-PET uptake and biodistribution in gliomas for neurosurgical planning and radiotherapy target delineation: pre-liminary results of a prospective pilot study. Int J Radiat Oncol. 2011; 81:S182–S182.

18. Asano S, Kameyama M, Oura A, Morisato A, Sakai H, Tabuchi Y, Chairoungdua A, Endou H, Kanai Y. l-type amino acid transporter-1 expressed in human astrocytomas, U343MGa. Biol Pharm Bull. 2007; 30:415–422. [PubMed: 17329830]

19. Soares-da-Silva P, Serrao MP. High- and low-affinity transport of l-leucine and l-DOPA by the hetero amino acid exchangers LAT1 and LAT2 in LLC-PK1 renal cells. Am J Physiol Renal Physiol. 2004; 287:F252–F261. doi:10.1152/ajprenal.00030.2004. [PubMed: 15271688]

20. Kuhne A, Tzvetkov MV, Hagos Y, Lage H, Burckhardt G, Brockmoller J. Influx and efflux transport as determinants of melphalan cytotoxicity: resistance to melphalan in MDR1 overexpressing tumor cell lines. Biochem Pharmacol. 2009; 78:45–53. doi:10.1016/j.bcp.2009.03.026. [PubMed: 19447222]

21. Kim CH, Park KJ, Park JR, Kanai Y, Endou H, Park JC, Kim do K. The RNA interference of amino acid transporter LAT1 inhibits the growth of KB human oral cancer cells. Anticancer Res. 2006; 26:2943–2948. [PubMed: 16886618]

22. Kumakura Y, Vernaleken I, Grunder G, Bartenstein P, Gjedde A, Cumming P. PET studies of net blood-brain clearance of FDOPA to human brain: age-dependent decline of [18F]fluoro-dopamine storage capacity. J Cereb Blood Flow Metab. 2005; 25:807–819. doi:10.1038/sj.jcbfm.9600079. [PubMed: 15729292]

23. Bauer R, Brust P, Walter B, Vorwieger G, Bergmann R, Fuchtner F, Steinbach J, el-Hallag E, Fritz A, Johannsen B, Zwiener U. Relation between brain tissue pO2 and dopamine synthesis of basal ganglia—a 18FDOPA-PET study in newborn piglets. J Perinat Med. 2000; 28:54–60. doi:10.1515/JPM.2000.008. [PubMed: 10765515]

24. Beuthien-Baumann B, Bredow J, Burchert W, Fuchtner F, Bergmann R, Alheit HD, Reiss G, Hliscs R, Steinmeier R, Franke WG, Johannsen B, Kotzerke J. 3-*O*-methyl-6-[18F]fluoro-l-DOPA and its evaluation in brain tumour imaging. Eur J Nucl Med Mol Imaging. 2003; 30:1004–1008. doi:10.1007/s00259-003-1205-2. [PubMed: 12768333]

25. Lennernas H, Nilsson D, Aquilonius SM, Ahrenstedt O, Knutson L, Paalzow LK. The effect of l-leucine on the absorption of levodopa, studied by regional jejunal perfusion in man. Br J Clin Pharmacol. 1993; 35:243–250. [PubMed: 8471400]

26. Morimoto E, Kanai Y, Kim do K, Chairoungdua A, Choi HW, Wempe MF, Anzai N, Endou H. Establishment and characterization of mammalian cell lines stably expressing human l-type amino acid transporters. J Pharmacol Sci. 2008; 108:505–516. [PubMed: 19075510]

27. Ichinoe M, Mikami T, Yoshida T, Igawa I, Tsuruta T, Nakada N, Anzai N, Suzuki Y, Endou H, Okayasu I. High expression of l-type amino-acid transporter 1 (LAT1) in gastric carcinomas: comparison with non-cancerous lesions. Pathol Int. 2011; 61:281–289. doi:10.1111/j.1440-1827.2011.02650.x. [PubMed: 21501294]

28. Kaira K, Oriuchi N, Imai H, Shimizu K, Yanagitani N, Sunaga N, Hisada T, Ishizuka T, Kanai Y, Endou H, Nakajima T, Mori M. l-type amino acid transporter 1 (LAT1) is frequently expressed in thymic carcinomas but is absent in thymomas. J Surg Oncol. 2009; 99:433–438. doi:10.1002/jso.21277. [PubMed: 19347882]

29. Kaira K, Oriuchi N, Shimizu K, Imai H, Tominaga H, Yanagitani N, Sunaga N, Hisada T, Ishizuka T, Kanai Y, Oyama T, Mori M, Endo K. Comparison of l-type amino acid transporter 1 expression and l-[3-18F]-alpha-methyl tyrosine uptake in outcome of non-small cell lung cancer. Nucl Med Biol. 2010; 37:911–916. doi:10.1016/j.nucmedbio.2010.06.004. [PubMed: 21055621]

30. Kobayashi H, Ishii Y, Takayama T. Expression of l-type amino acid transporter 1 (LAT1) in esophageal carcinoma. J Surg Oncol. 2005; 90:233–238. doi:10.1002/jso.20257. [PubMed: 15906366]

31. Nakanishi K, Matsuo H, Kanai Y, Endou H, Hiroi S, Tominaga S, Mukai M, Ikeda E, Ozeki Y, Aida S, Kawai T. LAT1 expression in normal lung and in atypical adenomatous hyperplasia and adenocarcinoma of the lung. Virchows Arch. 2006; 448:142–150. doi:10.1007/s00428-005-0063-7. [PubMed: 16175382]

32. Nakanishi K, Ogata S, Matsuo H, Kanai Y, Endou H, Hiroi S, Tominaga S, Aida S, Kasamatsu H, Kawai T. Expression of LAT1 predicts risk of progression of transitional cell carcinoma of the upper urinary tract. Virchows Arch. 2007; 451:681–690. doi:10.1007/s00428-007-0457-9. [PubMed: 17622555]

33. Sakata T, Ferdous G, Tsuruta T, Satoh T, Baba S, Muto T, Ueno A, Kanai Y, Endou H, Okayasu I. l-type amino-acid transporter 1 as a novel biomarker for high-grade malignancy in prostate cancer. Pathol Int. 2009; 59:7–18. doi:10.1111/j.1440-1827.2008.02319.x. [PubMed: 19121087]

34. Ebara T, Kaira K, Saito J, Shioya M, Asao T, Takahashi T, Sakurai H, Kanai Y, Kuwano H, Nakano T. l-type amino-acid transporter 1 expression predicts the response to preoperative hyperthermo-chemoradiotherapy for advanced rectal cancer. Anticancer Res. 2010; 30:4223–4227. [PubMed: 21036745]

35. Boado RJ, Li JY, Tsukamoto H, Pardridge WM. Hypoxia induces de-stabilization of the LAT1 large neutral amino acid transporter mRNA in brain capillary endothelial cells. J Neurochem. 2003; 85:1037–1042. [PubMed: 12716435]

36. Kaira K, Oriuchi N, Takahashi T, Nakagawa K, Ohde Y, Okumura T, Murakami H, Shukuya T, Kenmotsu H, Naito T, Kanai Y, Endo M, Kondo H, Nakajima T, Yamamoto N. LAT1 expression is closely associated with hypoxic markers and mTOR in resected non-small cell lung cancer. Am J Transl Res. 2011; 3:468–478. [PubMed: 22046488]

37. Cohen A, Hall MN. An amino acid shuffle activates mTORC1. Cell. 2009; 136:399–400. doi:10.1016/j.cell.2009.01.021. [PubMed: 19203575]

38. Wang Q, Bailey CG, Ng C, Tiffen J, Thoeng A, Minhas V, Lehman ML, Hendy SC, Buchanan G, Nelson CC, Rasko JE, Holst J. Androgen receptor and nutrient signaling pathways coordinate the demand for increased amino acid transport during prostate cancer progression. Cancer Res. 2011; 71:7525–7536. doi:10.1158/0008-5472.CAN-11-1821. [PubMed: 22007000]

39. Roos S, Kanai Y, Prasad PD, Powell TL, Jansson T. Regulation of placental amino acid transporter activity by mammalian target of rapamycin. Am J Physiol Cell Physiol. 2009; 296:C142–C150. doi:10.1152/ajpcell.00330.2008. [PubMed: 18987252]

40. Kim CS, Cho SH, Chun HS, Lee SY, Endou H, Kanai Y, Kim do K. BCH, an inhibitor of system l amino acid transporters, induces apoptosis in cancer cells. Biol Pharm Bull. 2008; 31:1096–1100. [PubMed: 18520037]

41. Imai H, Kaira K, Oriuchi N, Shimizu K, Tominaga H, Yanagitani N, Sunaga N, Ishizuka T, Nagamori S, Promchan K, Nakajima T, Yamamoto N, Mori M, Kanai Y. Inhibition of l-type amino acid transporter 1 has antitumor activity in non-small cell lung cancer. Anticancer Res. 2010; 30:4819–4828. [PubMed: 21187458]

42. Oda K, Hosoda N, Endo H, Saito K, Tsujihara K, Yamamura M, Sakata T, Anzai N, Wempe MF, Kanai Y, Endou H. l-type amino acid transporter 1 inhibitors inhibit tumor cell growth. Cancer Sci. 2010; 101:173–179. doi:10.1111/j.1349-7006.2009.01386.x. [PubMed: 19900191]
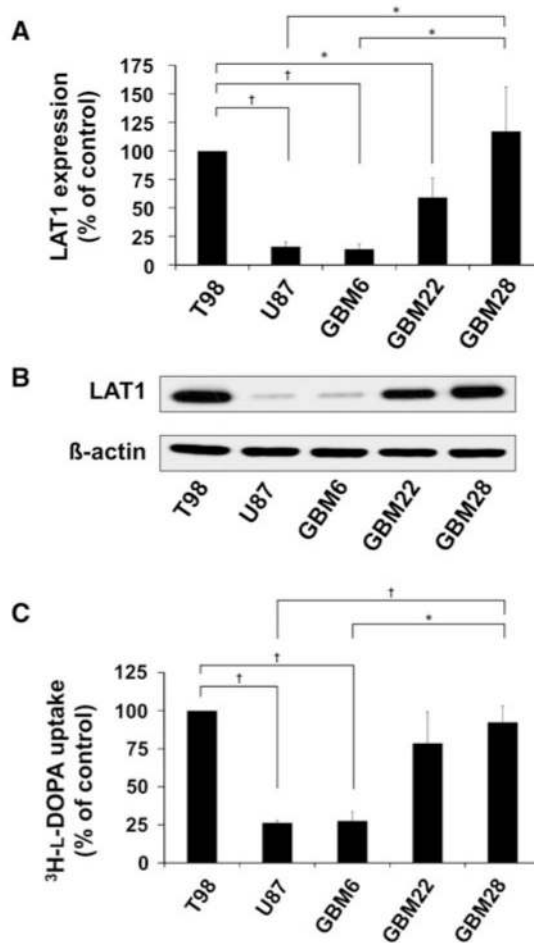
Fig. 1.
Endogenous LAT1 expression correlates with ^{3}H-L-DOPA uptake in GBM. Expression of
LAT1 **a** mRNA by qRT-PCR and **b** protein by Western blotting is shown for the indicated 5
tumor lines. **c** Uptake of ^{3}H-L-DOPA was evaluated in vitro. Both the qRT-PCR and uptake
studies are normalized to T98 cells as a control and data are plotted as mean of at least three
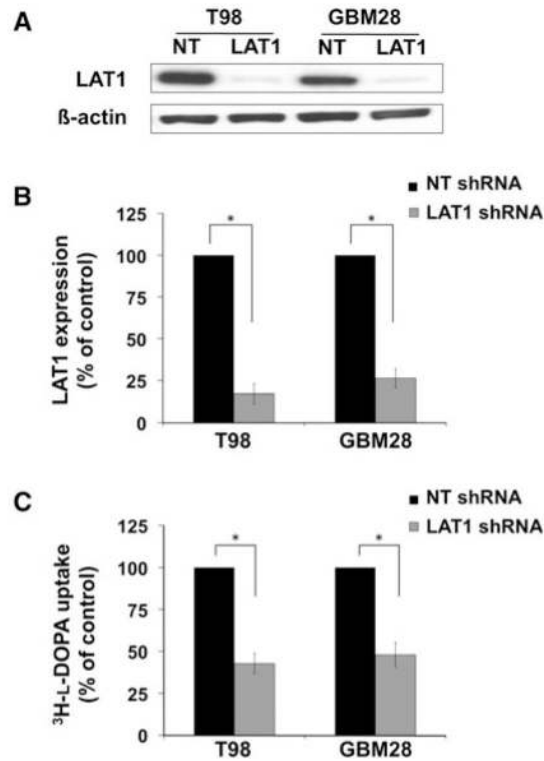independent experiments. Error bars are the standard error of the mean. (* P < 0.05; † P <
0.01)

Fig. 2.
Lentivirally delivered anti-LAT1 shRNA reduces ^{3}H-L-DOPA uptake (b). Data shown represents uptake in GBM. T98 and GBM28 were transduced with anti-LAT1 shRNA or with non-targeting (NT) shRNA controls. Reduced protein levels are seen on Western blots (**a**) and reduced mRNA is seen on qRT-PCR (**b**). Knockdown of LAT1 significantly reduced ^{3}H-L-DOPA uptake in both T98 and GBM28 (c). The data shown represents at least three independent experiments. Data are plotted as the mean ± SE of the mean of independent experiments with results normalized to NT shRNA vector transduced cells (* *P* < 0.001)
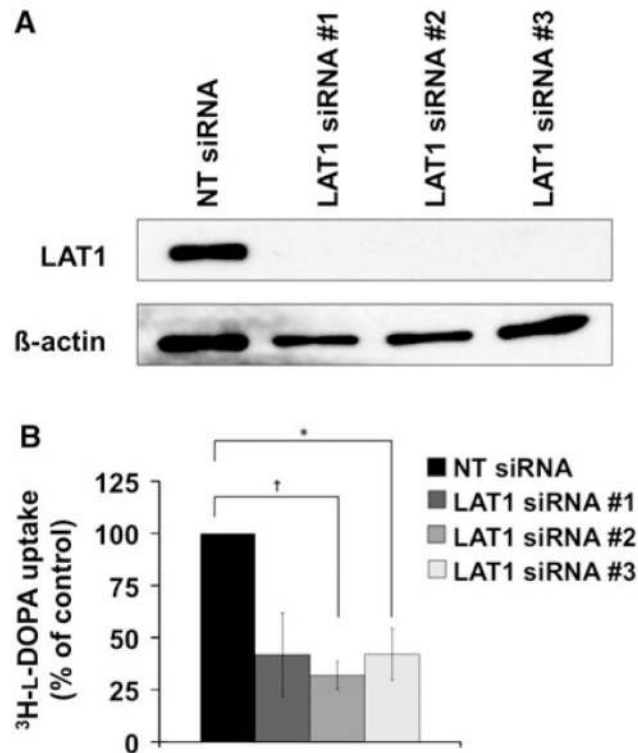
Fig. 3.
RNA interference by three anti-LAT1 siRNA sequences reduce ^{3}H-$_L$-DOPA uptake in GBM. Robust protein knockdown (**a**) was achieved in T98 cells transfected with anti-LAT1 siRNA compared with NT siRNA at 72 h. Reduction in LAT1 expression correlates with lower ^{3}H-$_L$-DOPA uptake (**b**). Data shown represents three independent experiments. Data are plotted as the mean ± SE of the mean of independent experiments with results normalized to NT siRNA vector transfected cells (* $P < 0.05$; † $P < 0.01$)
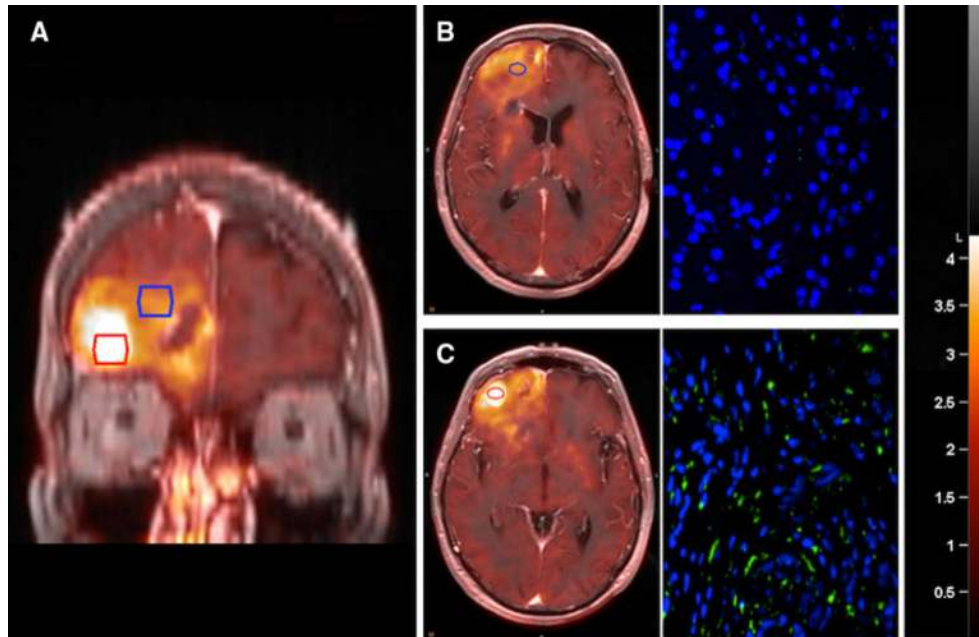
Fig. 4.
LAT1 expression correlates with ^{18}F-DOPA SUVmedian in newly diagnosed human astrocytoma. Biopsy samples were taken from regions of high (*red outlined region*) and low (*blue outlined region*) ^{18}F-DOPA uptake (**a**). Samples were then stained for LAT1 using immunofluorescence (*green*, Cy5-Lat1; *blue*, DAPI-nuclei). Regions of low (**b**) or high (**c**) ^{18}F-DOPA uptake demonstrated corresponding low and high LAT1 expression, respectively
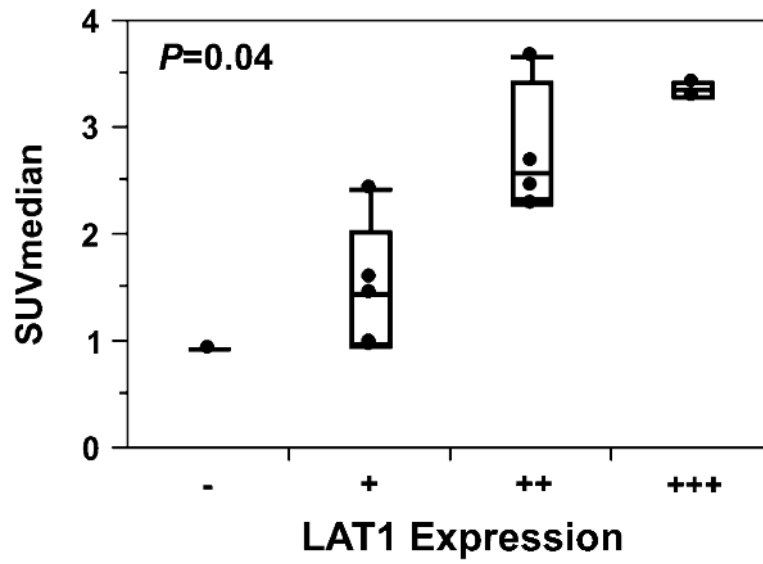
Fig. 5.
Semi-quantitatively graded LAT1 expression was statistically significantly correlated with ^{18}F-DOPA SUVmedian by Mann–Whitney U test ($P = 0.04$)